Optimization of Radio-Frequency Ion Thruster Discharge Chamber Using an Analytical Model

Emre Turkoz, Murat Celik*
Department of Mechanical Engineering
Bogazici University
Istanbul, Turkey

***Abstract*— The radio frequency ion thruster is an impulse generator to be used in space missions. It is a plasma based generator which utilizes electrostatic field between grids to accelerate the ionized gas out of the thruster to generate thrust. An analytical model is used to optimize the geometry of the discharge chamber which contains the inductively coupled plasma. The model is implemented and verified with existing thrusters and the results of the optimization process are presented. The results of our optimization routine validate the recent trend in radio frequency thruster design, which promotes hemispherical discharge chambers.**

Keywords—*electric propulsion, radio-frequency ion thrusters, inductively coupled plasma*

I. INTRODUCTION

The radio frequency (RF) ion engine, which is also known as RF ion thruster, is an impulse generator for small thrust values. It is among many plasma thrusters developed over the last few decades. As an electric propulsion system, the RF ion thruster relies on the acceleration of ionized gas to generate thrust. The ionization is provided by the energy carried by the RF waves in to the discharge chamber. The gas fed into the discharge chamber is Xenon.

The plasma thrusters are designed to provide a certain amount of thrust, which depends on the type of mission. The goal in thruster designs is to generate sustainable plasma with the required density for a specified thrust value, and to reduce the mean energy spent on the ionization of neutral gas. Reducing the mean ionization energy is related to the confinement of the particles, which would allow them to collide with each other in a more dense area and thus generate ions.

To understand the physics of the discharge chamber of an RF ion thruster, a numerical model is needed. Goebel [1] developed an analytical 0D model to calculate RF ion thruster performance and efficiency. Even though the model lacks spatial resolution, it manages to predict the performance of an RF thruster with good agreement. In this work, the analytical model developed in [1] is coupled with optimization routines to find the optimum chamber design and thruster parameters, which would result in minimum energy loss for maximum amount of ionization.

The design of the discharge chamber of RF ion thrusters is still evolving. First RF ion thrusters are developed by University of Giessen and Astrium GmbH under the name of the RIT's [2]. This family of ion thrusters consists of designs named according to their cylindrical chamber diameters. RIT-10 and RIT-15 [3] are members of this family, and they have 10 and 15 cm discharge diameters, respectively. The shape of the discharge chamber has evolved from a cylindrical shape to a conical one with RIT-XT [4]. The schematic of an RF ion thruster with a conical discharge chamber is given in Fig. 1. In one of the most recent designs, RIT-45 [5], the discharge chamber is hemispherical.

Our optimization scheme utilizes the model presented in [1] and evaluates these designs qualitatively in the course of finding the optimum design. There are many important parameters while evaluating the performance of an RF ion thruster. The current supplied to the RF coils generates a magnetic field which is inductively coupled with the plasma and confines the ions to prevent excessive loss to the walls. The electron number density, which is also called as the plasma density, is a key factor in determining the ionization collision frequencies. The screen area and the potential difference between the accelerator and the screen grid determine the amount of thrust to be generated. The interested reader is referred to [1] for further reading on the subject.

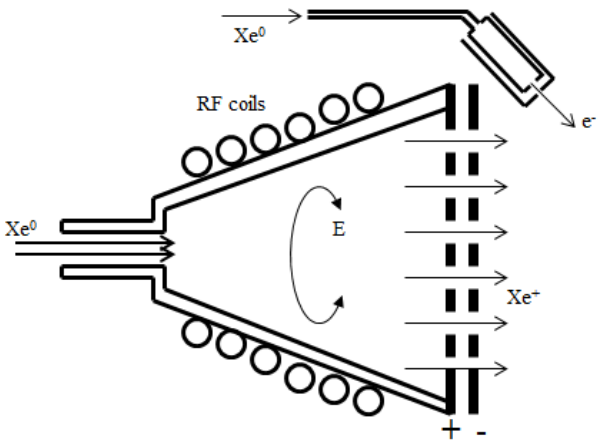

Fig. 1: The schematic of an RF ion thruster with a conical discharge chamber

*Corresponding author: Murat Celik
E-mail: murat.celik@boun.edu.tr

II. THE MODEL

In this section, the analytical model presented in [1] is first described shortly focusing on the input and the output parameters. Then the implementation is elaborated and the coupling with optimization routines is explained. Afterwards, the design parameters and objectives are clearly stated.

A. The 0D Analytical Model

The very detailed explanation of the model is presented in [1]. This model is implemented in this work. The most important output of the model is the discharge loss per ion, which is the measure of the mean energy spent to ionize one neutral particle in the discharge chamber. In our implementation, the model takes the chamber length, chamber base diameter, chamber top diameter, screen transparency and optical transparency values as inputs. As the result, alongside with the discharge loss per ion, our implementation gives confinement factor, plasma density, ion velocity and the magnetic field magnitude as the output for each mass utilization value.

The discharge loss per ion is found by dividing the input power by the ion beam current:

$$\eta_d = \frac{P_{abs}}{I_b} \tag{1}$$

where η_d is the discharge loss per ion, P_{abs} is the input power to the plasma and I_b is the beam current. Input power is calculated as follows [1]:

$$P_{abs} = I^{+}U^{+} + I^{++}U^{++} + I^{*}U^{*} + (I_s + I_w + I_b)\,(0.5T_e + \varphi) + I_a\,(2T_e + \varphi) \tag{2}$$

where U^{+} is the first ionization potential, U^{++} is the second ionization potential and U^{*} is the excitation potential. Similarly, I^{+} is the singly ionized particle production rate, I^{++} the double ionized particle production rate and I^{*} the excited neutral production rate. The potential values are specific for each type of gas used to generate the plasma. The production rates have similar expressions. The singly ionized particle production rate is [1]:

$$I^{+} = n_0 n_e e \left\langle \sigma_i^{+} v_e \right\rangle V \tag{3}$$

Similarly, the double ionized particle production rate is as follows:

$$I^{++} = n_e^2 e \left\langle \sigma_i^{++} v_e \right\rangle V \tag{4}$$

And, the excited neutral production rate is:

$$I^{*} = n_0 n_e e \left\langle \sigma^{*} v_e \right\rangle V \tag{5}$$

In these equations, n_0 denotes the neutral number density, n_e denotes the electron, and due to quasi neutrality, plasma number density. e is the elementary charge, σ^{+}, σ^{++} and σ^{*} are the first ionization, second ionization and excitation cross sections of Xenon, respectively, v_e denotes the electron velocity and V is the plasma volume.

Other terms that take part in the calculation of absorbed power are the ion current to the screen grid (I_s), to the wall (I_w), and the ion beam current that passes through the grids of the screen (I_b) [1]. The formulation of these terms is as follows:

$$I_s = \frac{(1 - T_s)}{2} n_i e v_a A_s \tag{6}$$

$$I_w = \frac{1}{2} n_i e v_a A_w f_c \tag{7}$$

$$I_b = \frac{1}{2} n_i e v_a A_s T_s \tag{8}$$

In these equations v_a denotes the ion acoustic velocity given by:

$$v_a = \sqrt{\frac{kT_e}{M}} \tag{9}$$

Also, f_c is the confinement factor, which indicates the ion current reaching the wall divided by the Bohm current. A_s is the grid area, and A_w is the wall area. n_i is the ion density which consists of the sum of the singly and doubly ionized particles. T_e is the electron temperature and M is the molar mass of the Xenon atoms. The only remaining term in the absorbed power equation is the floating potential, which is defined as [1]:

$$\varphi = \frac{kT_e}{e} \ln\left[\sqrt{\frac{2M}{\pi m}}\right] \tag{10}$$

Our implementation of the model requires some approximations. We assume that the screen grid transparency is known and it is taken as a constant value of 0.8. The optical transparency is actually calculated using ion optics physics. An example of ion optics numerical model is the CEX2D code developed in JPL [6]. An extension of this code in 3D is also developed again in JPL with the name CEX3D [7]. In this work, an ion optics code is not utilized. Instead, a first order approximation presented in [8] is utilized to calculate the optical transparency:

$$\phi_0 = \frac{1}{(1/\phi_{screen}) + (1/\phi_{accel}) - 1} \tag{11}$$

where ϕ_{screen} is screen grid transparency and ϕ_{accel} is the accelerator grid transparency. Farnell [9] laid out the conventional relationship between the screen and the accelerator grid transparencies in ion thrusters as follows:

$$\frac{\phi_{accel}}{\phi_{screen}} = 0.36 \tag{12}$$

This relation is utilized in this paper and the optical transparency is calculated with the formula presented. Another approximation is performed for the Clausing factor, which defines the reduced conductance of the grids with finite thicknesses. This factor is calculated using Monte Carlo techniques and it is typically on the order of 0.5 [1]. As an approximation this value is taken constant for all grid designs

as 0.5. In the reference study of this work [1], the coil current is taken to be constant as the discharge loss per ion value is assumed to be around 250 eV/ion. A similar approach is obtained in this work and a formula is used to calculate the coil current and the magnetic field. To develop this approach, the fact is utilized that the beam current is directly proportional to the impulse desired to be generated. Therefore the beam current value is held constant and the coil current is changed according to the following formula:

$$\eta_{coupling} I_{coil}^2 \Omega_{coil} = \Delta_{loss} I_{beam} \tag{13}$$

where I_{coil} is the coil current, I_{beam} is the beam current, Ω_{coil} is the coil impedance, Δ_{loss} is the discharge loss per ion and $\eta_{coupling}$ is the coupling efficiency of the coil and the plasma. The coil impedance is conventionally taken to be $50\,\Omega$. The discharge loss per ion value changes with mass utilization efficiency. As the coil current changes, the induced magnetic field also changes with the following relation:

$$B = \mu_0 N I_{coil} \tag{14}$$

where B is the induced magnetic field, μ_0 is the magnetic constant, N is taken constant with the value 100 turns/meter. Our implementation represents the model presented in [1] with some minor differences in parameter definitions. The model uses the balance of ion production and loss terms in the plasma to evaluate electron temperature. Ion production is also calculated to evaluate the discharge loss. To account for the ion production with higher accuracy, double ionization should also be brought into the picture. The data of reaction rate for double ionization for Xenon is obtained from [9]. To use the data, a nonlinear least square fit is performed on the data points using the following function template:

$$10^{-15}\left(\left(C + BT_{eV} + AT_{eV}{}^2\right)e^{-21.2/T_{eV}}\right)\sqrt{\frac{8\mathrm{eT_{eV}}}{\pi \mathrm{m}}} \tag{15}$$

where T_{eV} is electron temperature in electron volts, m is the electron mass, e is the elementary charge value. This form is similar to the form presented in [10] which is used to find the single ionization reaction rate. The result is evaluated as follows: A = 1.6113, B = 3.4056 and C = 1.5563. The single and double ionization reaction rates along with the excitation reaction rate are plotted in Fig. 2.

B. Implementation of the Model

The model is implemented in MATLAB. The optimization routine is executed with three input parameters. A conical discharge chamber is assumed. These parameters are the base and the screen (grid) diameters of the conical chamber and the axial length. The objective is to minimize the average discharge loss per ion for the mass utilization values ranging between 0.7 and 0.95. The lower and upper bounds of the three parameters are determined as follows: The base diameter values are subject to vary between 4 cm and 12 cm whereas the screen diameter is subject to vary between 8 cm and 28 cm. The chamber length can take values between 10 cm and 25 cm.

The appropriate values are picked by the optimization routine and these three values are given as inputs to the main routine of the algorithm. The main routine mainly consists of three nested loops. The geometry calculations are performed and the chamber volume and the chamber wall surface area are calculated. Then the routine enters the first loop over mass utilization values ranging from 0.7 to 0.95. In this loop there is a second loop for the induced magnetic field value. The induced magnetic field depends on the coil current which depends on the discharge loss per ion. Since the induced magnetic field also affects the discharge loss per ion, the loop monitors the convergence of the magnetic field for the discharge loss per ion value evaluated by the third loop. The third loop is the most computationally expensive part of the routine. The third loop monitors the convergence of the confinement factor. It starts with the calculation of the neutral number density which is a function of mass utilization efficiency, grid area and optical transparency. Then electron temperature is calculated with a trial-and-error approach. Values between 0.4 and 15 eV are tried and the value with the minimum error is picked as the electron temperature. The correct temperature values result with a sharp decline in the error function. The temperature values are plotted against the normalized error in an example trial and error case, which is to be seen in Fig. 3.

After the electron temperature is determined, the plasma conductivity, floating potential and electron-neutral collision frequencies are subsequently calculated. Then the electron number density is calculated with beam current, screen area, transparency values and electron temperature. For the last step the Bohm velocity is calculated using the electron temperature and the convergence criteria, the confinement factor is evaluated as the ratio of the ion velocity divided by the Bohm velocity. The loop iterates until the confinement factor converges to a value. The dependency of the important parameters in the third loop is presented in Fig. 4.

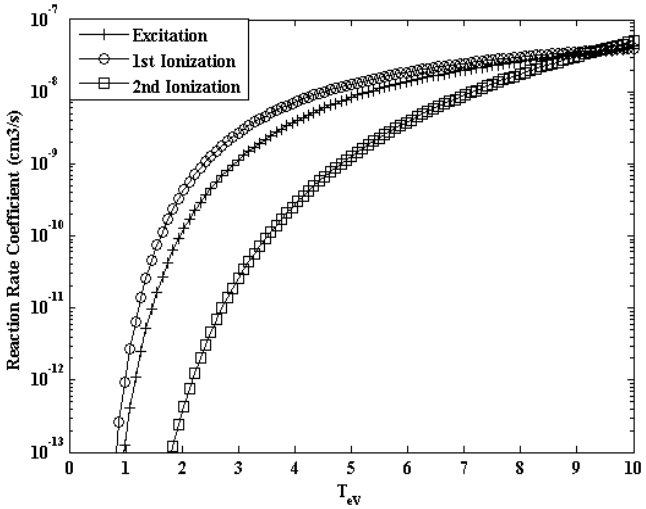

Fig. 2: Reaction rates for Xenon.

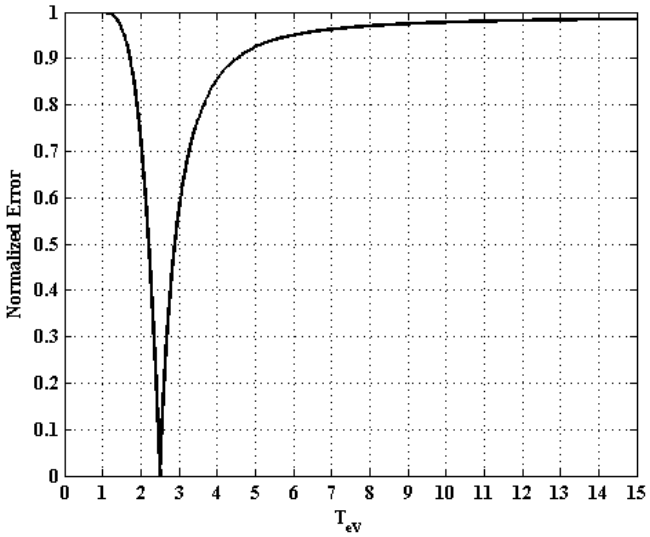

Fig. 3: Normalized error and electron temperature

III. RESULTS

A validation of the model was necessary before obtaining the optimization results. The validation is performed according to the data presented in [1]. After the implementation is validated, the results of the optimization are presented.

A. Validation

The validation is performed using the example case presented in [1]. This example conical discharge chamber has 10 cm chamber length, 22 cm screen diameter and 5 cm base diameter. The code is performed for three induced magnetic field values: 0 G, 6 G and 12.6 G. The results are plotted in Fig. 5. These results match with a high accuracy to those given in [1] and in accordance with the experimental results presented in [11] for RIT-22 ion engine in operating conditions (about 0.9 mass utilization efficiency). Fig. 5 shows three different cases for the different induced magnetic field values. The solid line represents the case with 0 G, i.e. no ion confinement. As expected the discharge loss per ion in the operation range is the highest. The dashed line represents the 6 G case and the dotted line with the lowest discharge loss per ion value represents the 12.6 G case.

B. Results of the Optimization

The optimization procedure yields the design parameters on the bounds. As the result of the optimization process, the ideal conical chamber configuration within the parameter bounds turns out to be 10 cm long, having 4 cm base diameter and 28 cm screen diameter. The discharge loss per ion against the mass utilization efficiency is plotted for this configuration and can be seen in Fig. 6. Different bounds yield the same tendency. In other words, the discharge loss per ion is minimum for the conical discharge chamber configuration if:

- The chamber length is as small as possible
- The base diameter is as small as possible
- The screen diameter is as large as possible

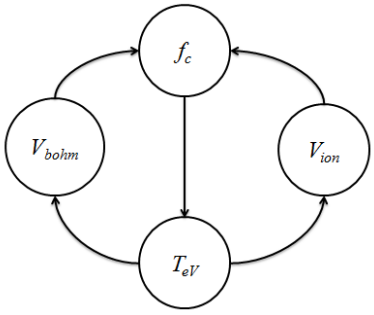

Fig. 4: Dependency scheme of the third loop

This result indicates that the smallest discharge loss per ion values can be obtained with the minimization of the wall area to reduce the ionization losses. On the other hand, the screen diameter is kept as large as possible. These "possible" bounds are determined according to the applicability of our model. Since the model is 0D, it assumes uniform properties throughout the plasma. The coil is a limitation while determining the chamber length, since very different chamber lengths with the same coil would result with different coil impedances which are not covered by the current model. Other limitation is on the grid diameter for the approximations made while evaluating the transparency values and the Clausing factor. Without addition of an ion optics code and a Monte Carlo solver, the screen diameter would better remain in the current bounds since the values are available from the literature for these values.

This tendency of the optimization routine indicates that the best configuration has the smallest surface area and the largest plasma volume. The recent designs [5] along with our findings lead to think that a hemispherical discharge chamber may have the best performance characteristics. A hemispherical design, which has the same discharge volume with the optimum conical design has 10.13 cm chamber length and radius. The results of the optimum conical design and the optimum hemispherical design are presented in Fig. 6 show that the discharge loss per ion is higher for the optimum conical design than the hemispherical design which has the same volume and the same grid diameter. The curve represented by the dashed lines denote the discharge loss per ion values for the hemispherical configuration whereas the solid line represents the optimum conical configuration for the same volume.

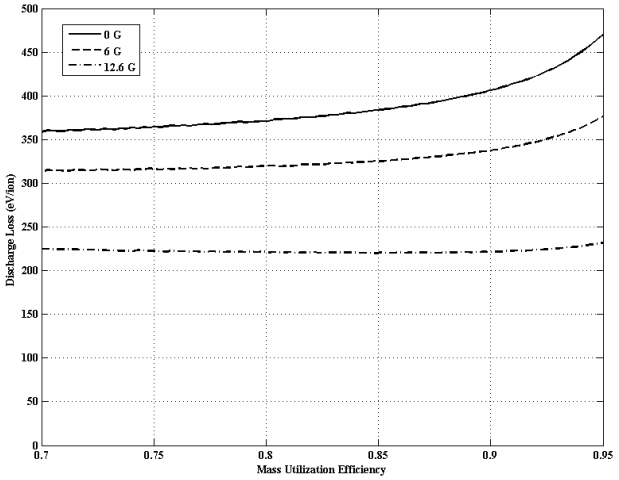

Fig. 5: Discharge loss per ion versus mass utilization efficiency for three different magnetic fields

IV. CONCLUSION

The analytical 0D model presented in [1] is successfully implemented and validated with the results presented in the same work. A self consistent iterative solution of the model is implemented. An optimization study is performed to minimize the average discharge loss per ion over reasonable mass utilization efficiencies. The parameters to be changed by the optimization routine are determined as the chamber length, base diameter and screen diameter. The result of the optimization indicates that the discharge loss per ion is minimized when the wall area of the discharge chamber is the smallest. This phenomenon and the latest trends in thruster design [5] lead us to conclude that better designs are possible with a hemispherical configuration, since sphere is the geometry which has the largest surface area to volume ratio. An example hemispherical configuration which has the same chamber volume with the optimum conical configuration is evaluated and this claim is validated.

Even though our implementation has an accurate tendency and capability to be used for a thruster design, some improvements are required for better accuracy. An ion optics code can be incorporated into the implementation, so the grid transparency can better be evaluated with the changing grid diameter. A Monte Carlo solver may also prove to be useful to calculate the Clausing factor. Also the reaction rates and the collision frequencies are evaluated with the cross-section data for Xenon. This data are evaluated experimentally and the results are embedded in the code. If a different gas is desired to be used, the necessary experimental data again should be fed into the code. The 0D model assumes constant properties throughout the chamber volume. The development of a 2D model would prove to be very useful in thruster design to observe the local variations and evaluate the discrete parameter values.

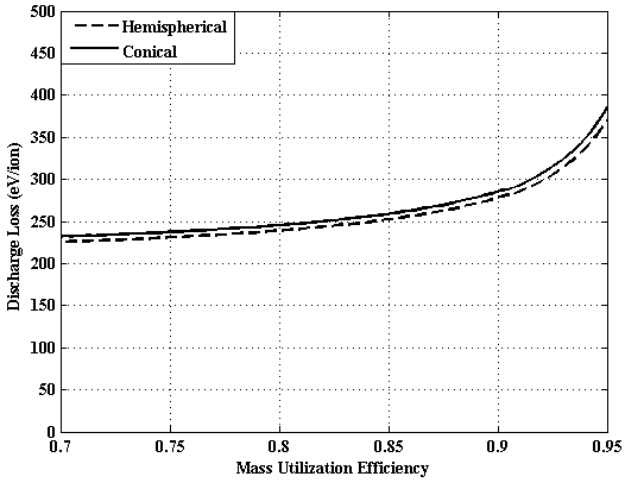

Fig. 6: Discharge loss per ion versus mass utilization efficiency for the optimum conical and the corresponding hemispherical design which have the same discharge volumes and the grid diameter

REFERENCES

[1] D. M. Goebel, "Analytical discharge model for RF ion thrusters," IEEE transactions on plasma science, vol. 36, no. 5, October 2008.

[2] H. Bassner, R. Killinger, H.Leiter, and J.Müller, "Development steps of the RF-ion thrusters RIT," 27th International Electric Propulsion Conference, 2001, IEPC-01-105.

[3] K. H. Loeb, H. J. Leiter, and H. W. Loeb, "RIT 15 – A medium range radio-frequency ion thruster," 2nd European Space Propulsion Conference, 1997, 1997ESASP.398.377G.

[4] H. J. Leiter, R. Killinger, H. Bassner, J. Müller, R. Kukies, and T. Fröhlich, "Evaluation of the performance of the advanced 200 mN radio frequency ion thruster RIT-XT," 38th Joint Propulsion Conference, Indianapolis, Indiana, July 7-10, 2002, AIAA-2002-3836.

[5] H. W. Loeb, D. Feili, G. A. Popov, V. A. Obukhov, V. V. Balashov, A. I. Mogulkin, V. M. Murashko, A. N. Nesterenko, and S. Khartov, "Design of high-power high-specific impulse RF-ion thruster," 32nd International Electric Propulsion Conference, 2011, Wiesbaden, Germany, IEPC-2011-290.

[6] J. R. Brophy, I. Katz, J. E. Polk, and J. R. Anderson, "Numerical simulations of ion thruster accelerator grid erosion," 38th Joint Propulsion Conference and Exhibit, 2002, Indianapolis, IN, USA, AIAA-2002-4261.

[7] J. R. Anderson, I. Katz, and D. M. Goebel, "Numerical simulation of two-grid ion optics using a 3D code," 40th Joint Propulsion Conference, 2004, Fort Lauderdale, Florida.

[8] M. Tsay, "Two-dimensional numerical modeling of Radio-Frequency ion engine discharge," Thesis (Ph. D.) – Massachusetts Institute of Technology, Dept. of Aeronautics and Astronautics, 2010.

[9] E. W. Bell, "Electron-impact ionization of In and Xe," Physical Review A, vol. 48, no. 6, December 1993.

[10] D. M. Goebel, I. Katz, "Fundamentals of Electric Propulsion – Ion and Hall Thrusters," JPL Space Science and Technology Series, March 2008.

[11] H. Leiter, R. Kukies, R. Killinger, E. Bonelli, S. Scaranzin, and F. Scortecci, "RIT-22 ion engine development—Endurance test and life prediction," presented at the 42nd Joint Propulsion Conf., Sacramento, CA, Jul. 9–12, 2006, Paper No. AIAA-2006-4667.